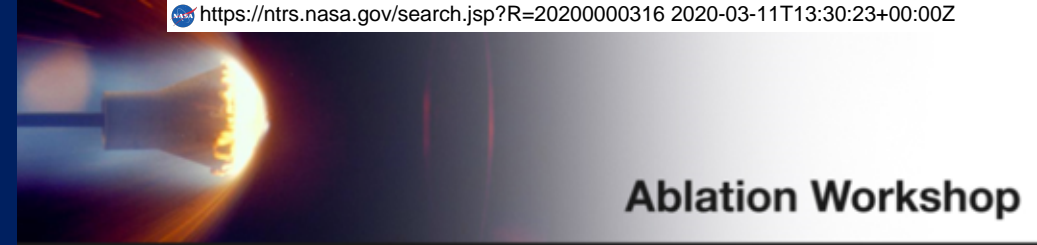Ablation Workshop

Computation of fiber orientation in X-ray micro-tomography reconstructions

Presented by Federico Semeraro

Monday 16th September 2019

Authors: Federico Semeraro[1], Joseph C. Ferguson[1], Francesco Panerai[2], Nagi N. Mansour[3]

1. Science and Technology Corp. at NASA Ames Research Center, Moffett Field, CA 94035
2. Department of Aerospace Engineering, University of Illinois at Urbana-Champaign, IL 61801
3. NASA Ames Research Center, Mail Stop 258-5, Moffett Field, CA 94035

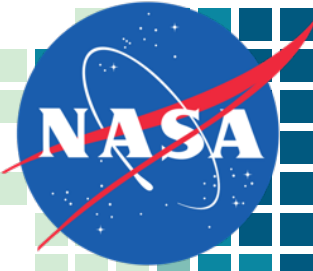## Technical Session #1:
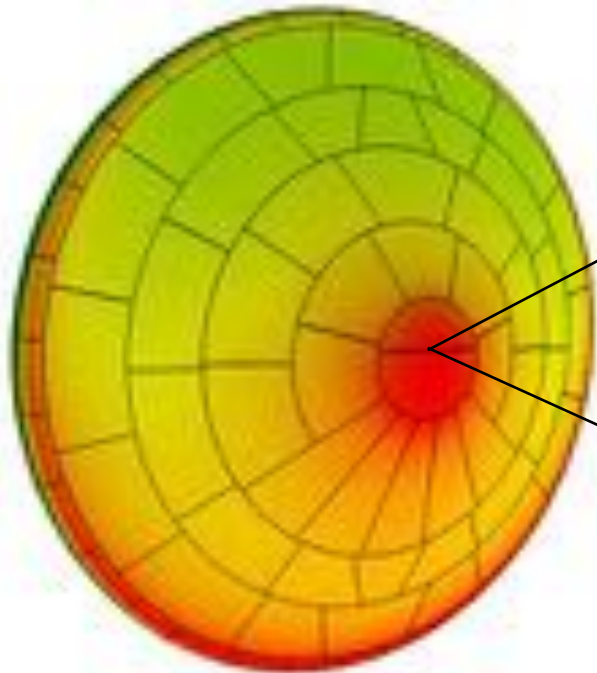## Micro-tomography based analysis
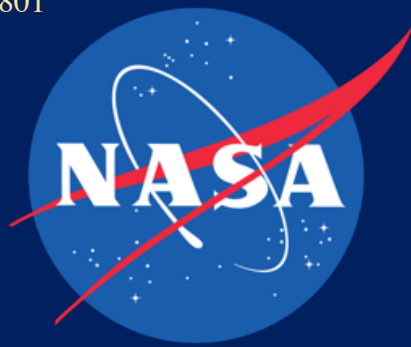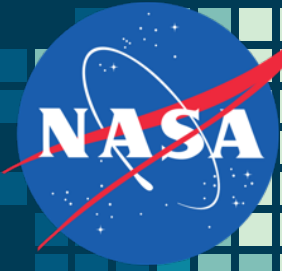
MOTIVATION & OBJECTIVES

# Modeling Thermal Protection Systems (TPS)

Macroscale Modeling

Full scale material response solvers, using volume-averaged techniques to solve conservation equations for ablation

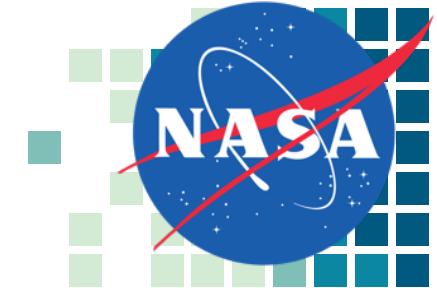Simulation of surface temperature for MSL heatshield[1]

Microscale Modeling

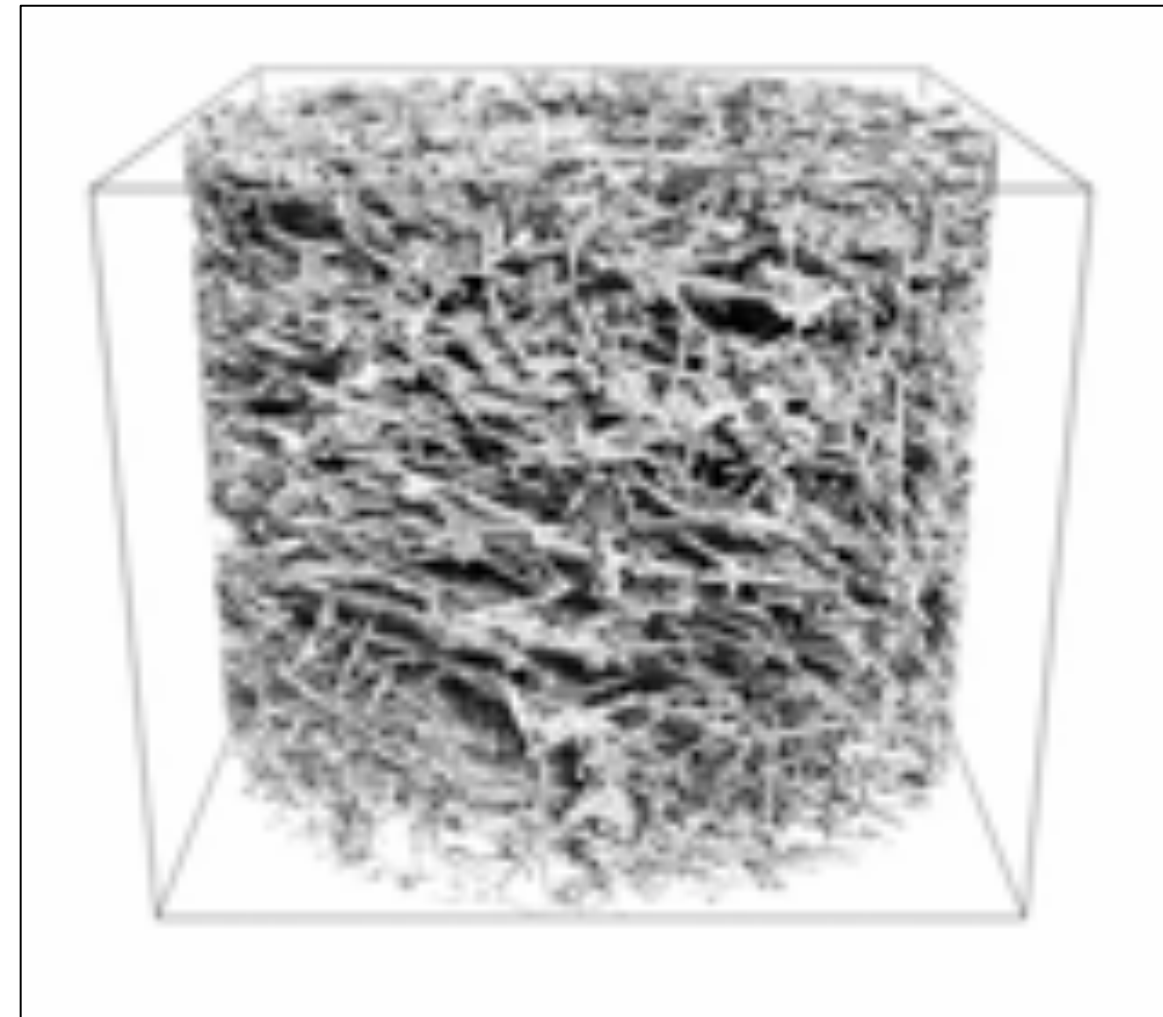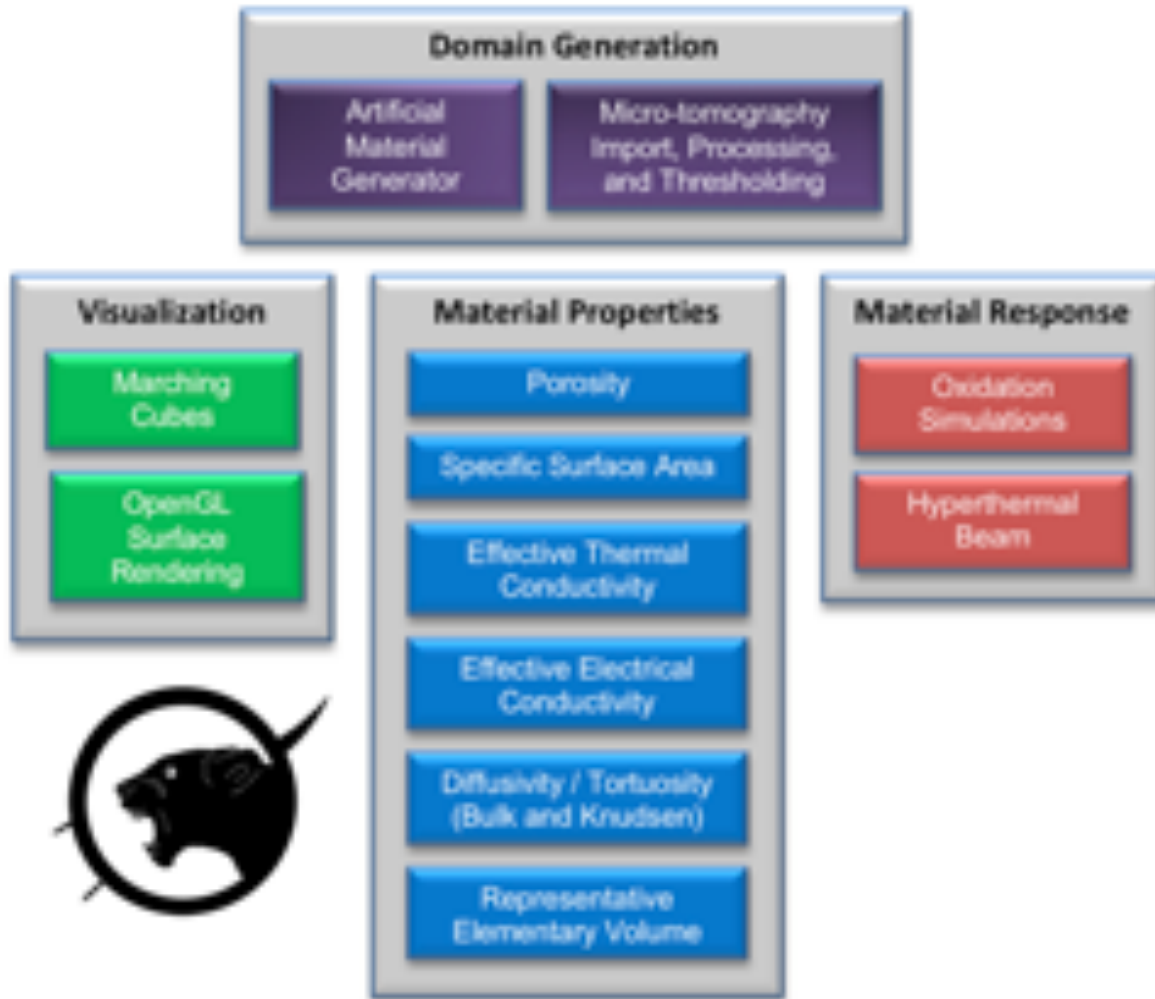Used to inform material properties and material response parameters used in macro-scale modeling
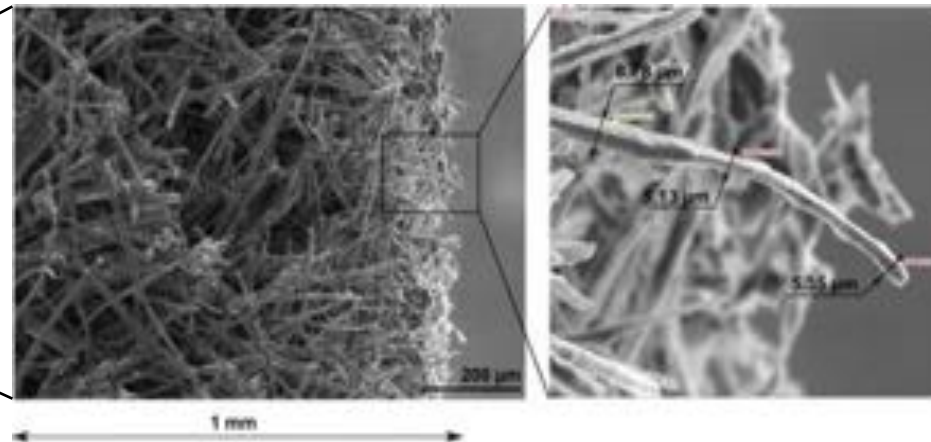
Lachaud and Mansour, *JTHT* 2013

[1] Meurisse, Jeremie BE, et al. "Multidimensional material response simulations of a full-scale tiled ablative heatshield." *Aerospace Science and Technology 76 (2018)*: 497-511.

3

Porous Microstructure Analysis (PuMA)

Domain Generation
- Artificial Material Generator
- Micro-tomography Import, Processing, and Thresholding

Visualization
- Marching Cubes
- OpenGL Surface Rendering

Material Properties
- Porosity
- Specific Surface Area
- Effective Thermal Conductivity
- Effective Electrical Conductivity
- Diffusivity / Tortuosity (Bulk and Knudsen)
- Representative Elementary Volume

Material Response
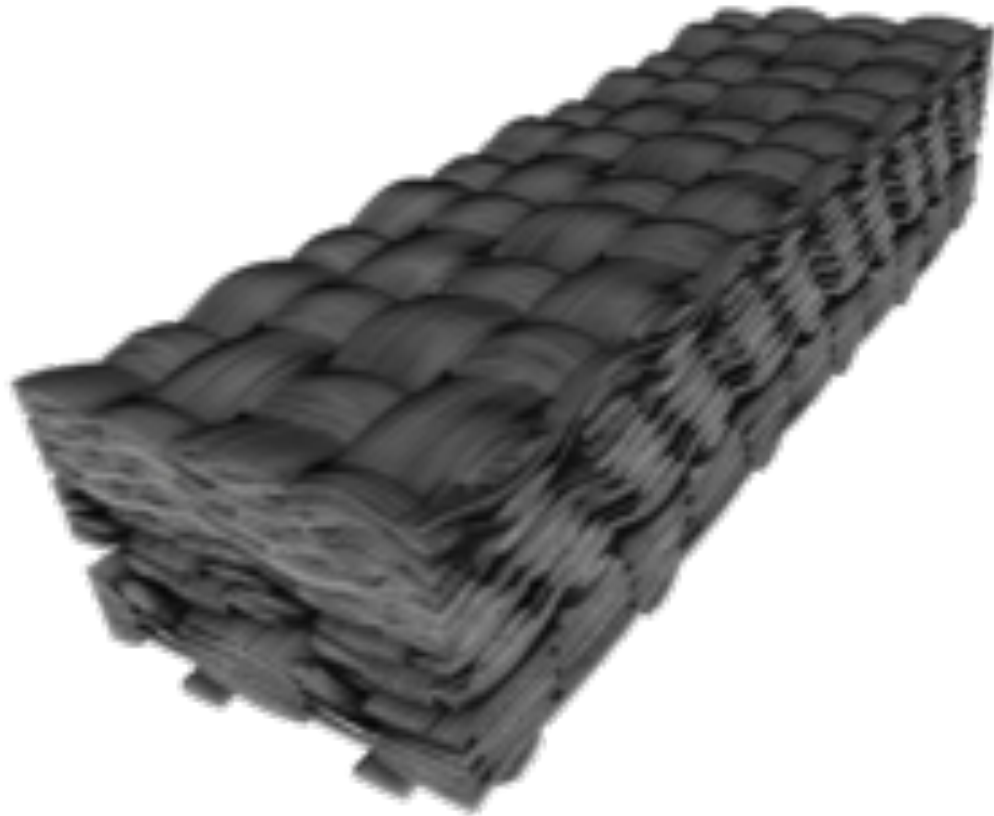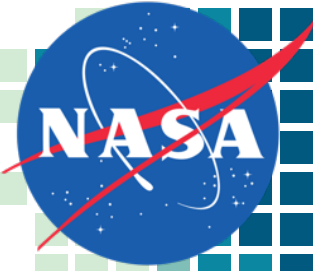- Oxidation Simulations
- Hyperthermal Beam

CT Reconstruction of FiberForm

Ferguson, J. C., Panerai, F., Borner, A., & Mansour, N. N. (2018). PuMA: the Porous Microstructure Analysis software. *SoftwareX*, *7*, 81-87.
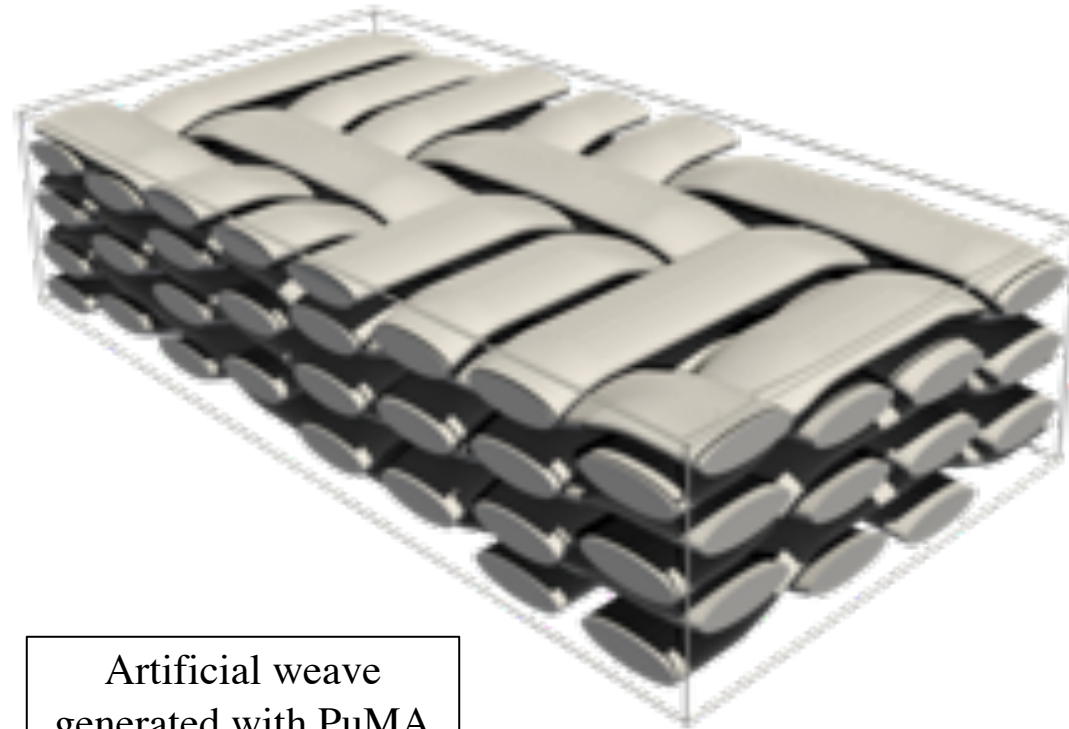https://software.nasa.gov/software/ARC-17920-1
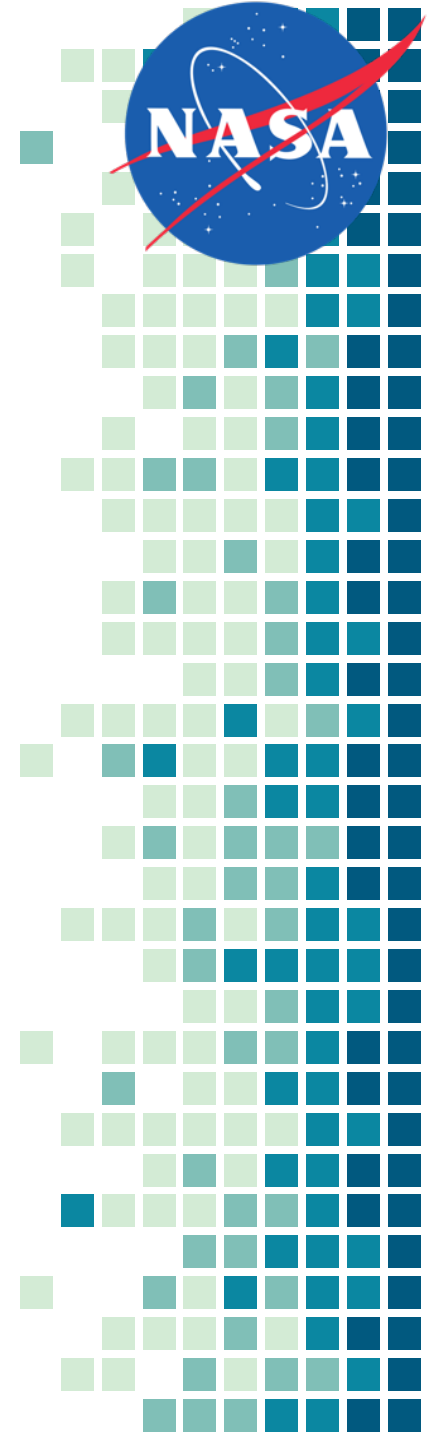
4

Challenges in Micro-scale modeling

12-ply real
TPS weave

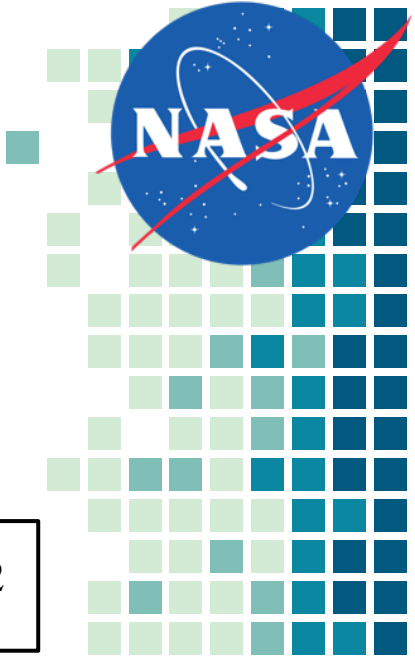As NASA moves towards
woven TPS materials, our
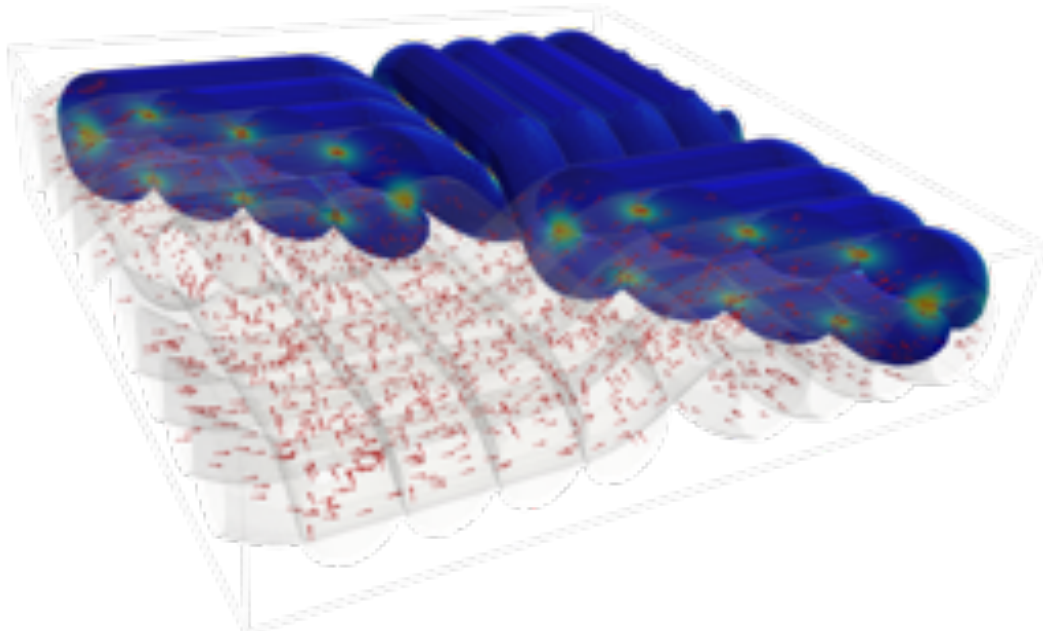modeling must adapt
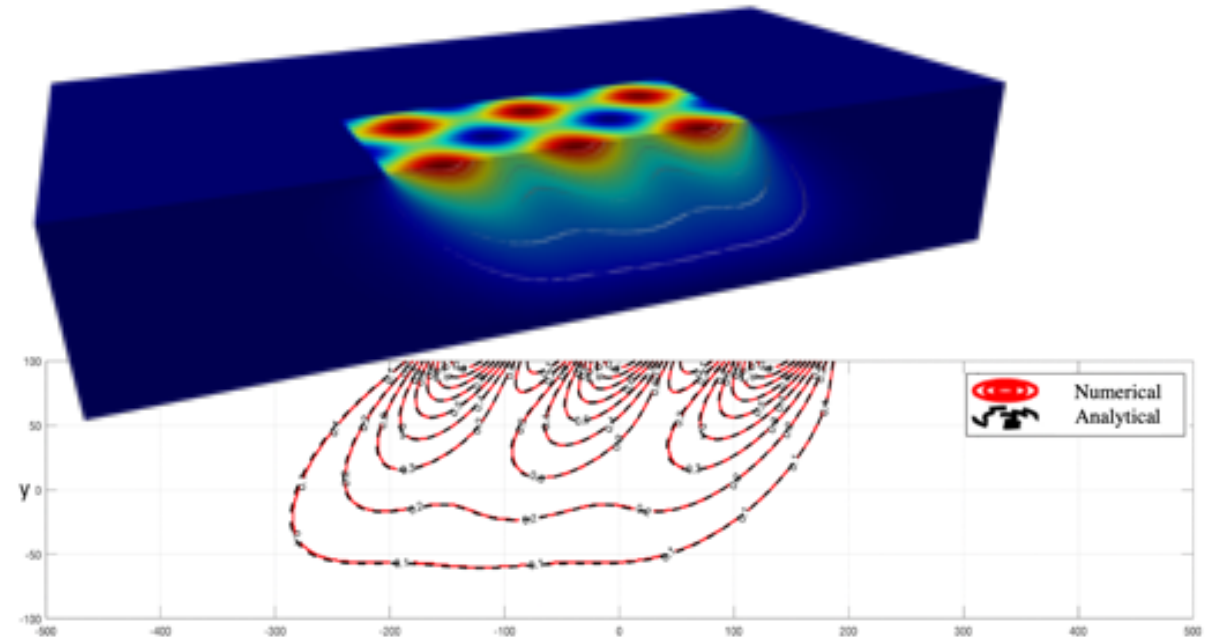
Artificial weave
generated with PuMA

Objectives

Computation of Effective Material Properties

Fiber Orientation Estimation[1]

Physical and Numerical Model[2]

[1] Federico Semeraro, Joseph C. Ferguson, Francesco Panerai, Robert J. King, Nagi N. Mansour. Anisotropic Analysis of Fibrous and Woven Porous Media, Part I: Estimation of Local Material Orientation. *Journal of Computational Physics [to appear]*
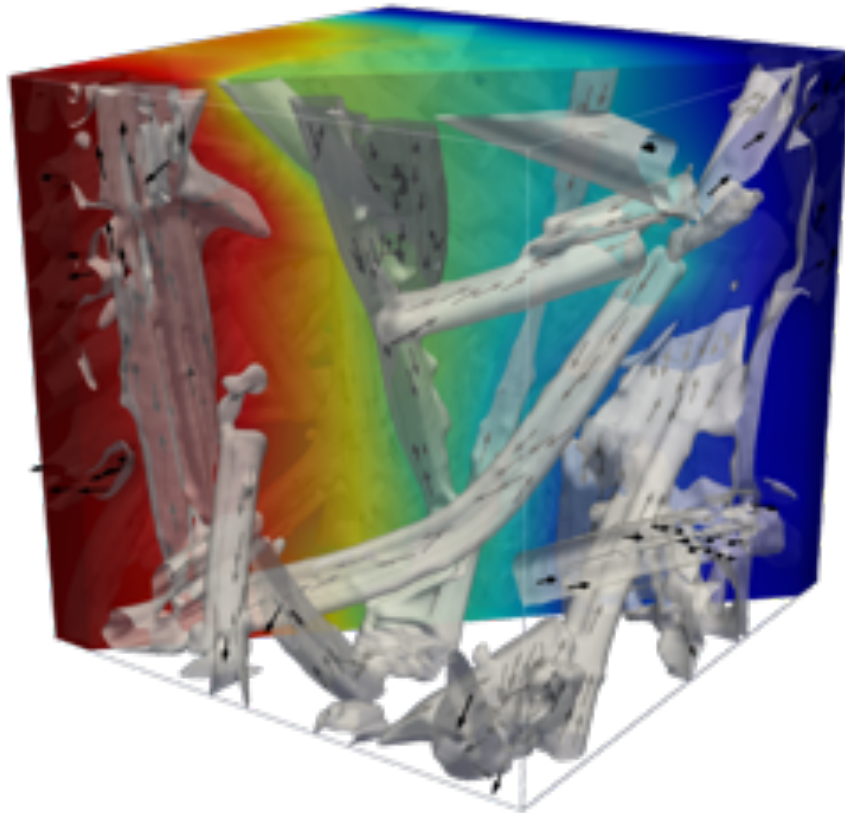
[2] Federico Semeraro, Joseph C. Ferguson, Francesco Panerai, Nagi N. Mansour. Anisotropic Analysis of Fibrous and Woven Porous Media, Part II: Computation of Effective Conductivity. *Journal of Computational Physics [to appear]*
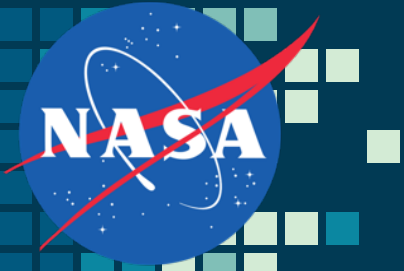
FIBER ORIENTATION METHODS
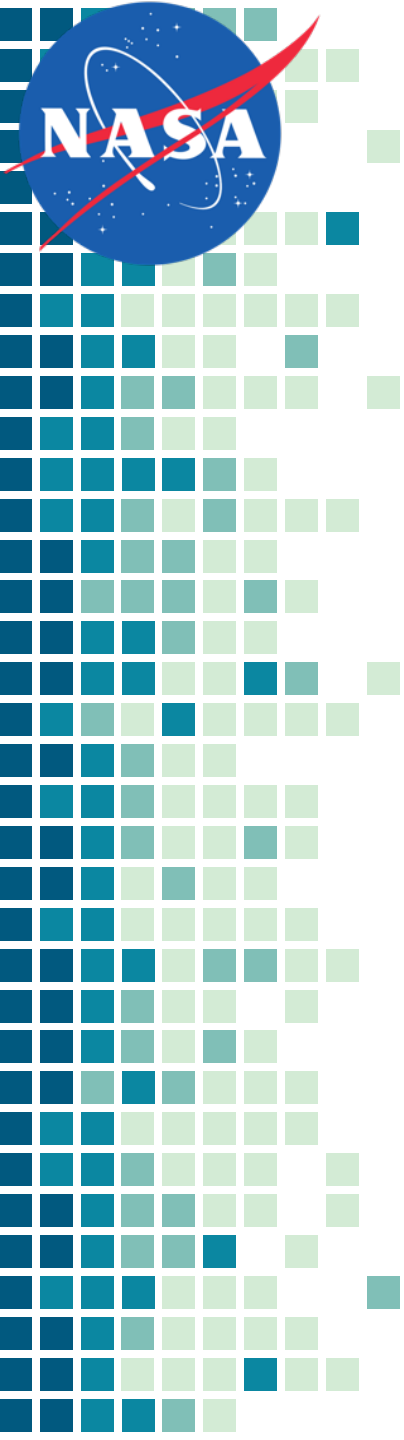
Overview

- Ray Casting (novel)

- Artificial Flux[1]
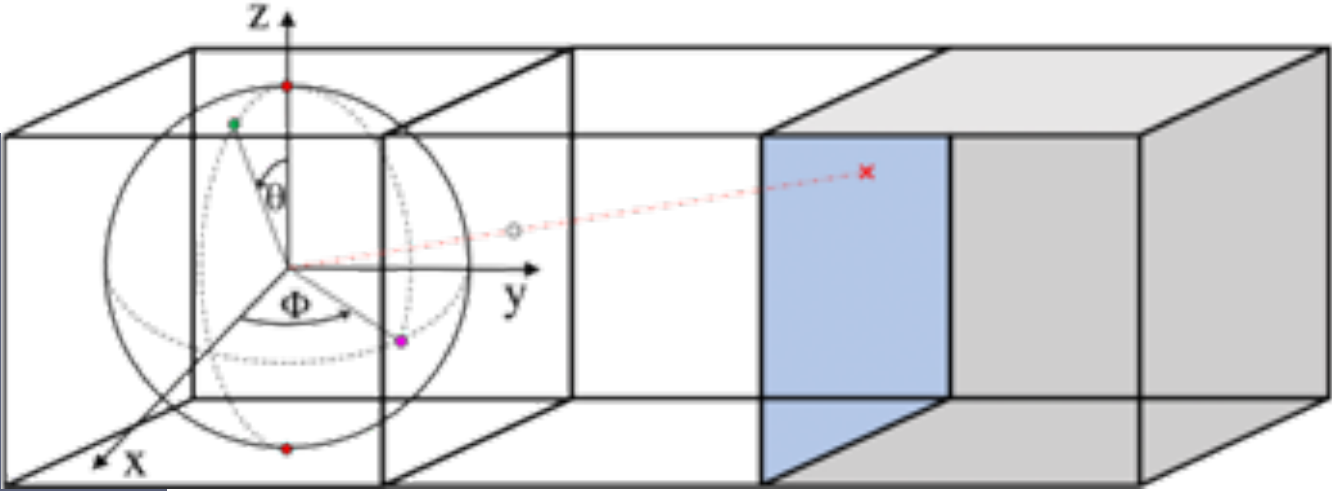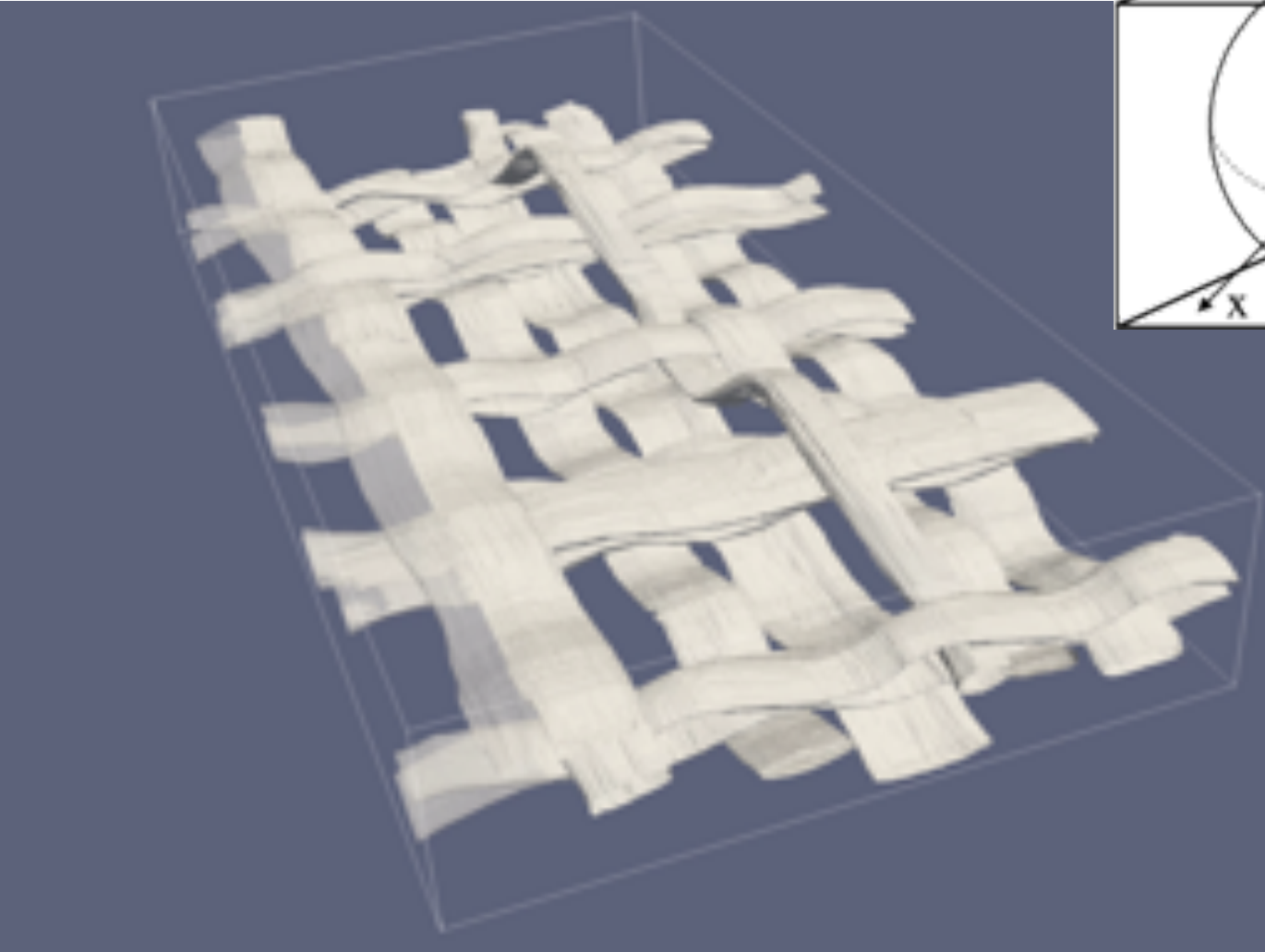
- Structure Tensor[2]

[1] Matti Schneider, Matthias Kabel, Heiko Andrä, et al. Thermal fiber orientation tensors for digital paper physics. *International Journal of Solids and Structures 2016*; 100-101 234

[2] Krause M, Hausherr JM, Burgeth B, Herrmann C, Krenkel W. Determination of the fibre orientation in composites using the structure tensor and local x-ray transform. *J Mater Sci 2010*; 45(4):888–96.
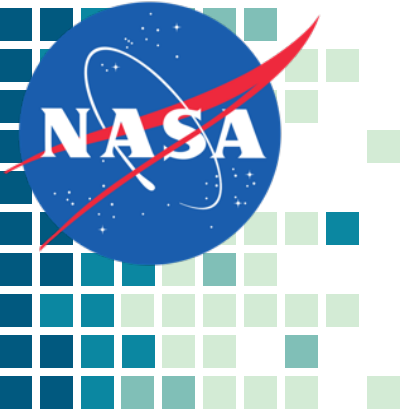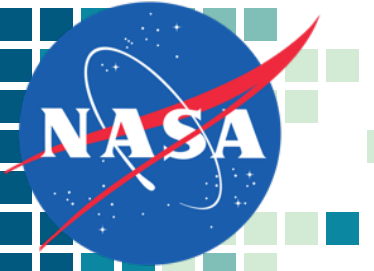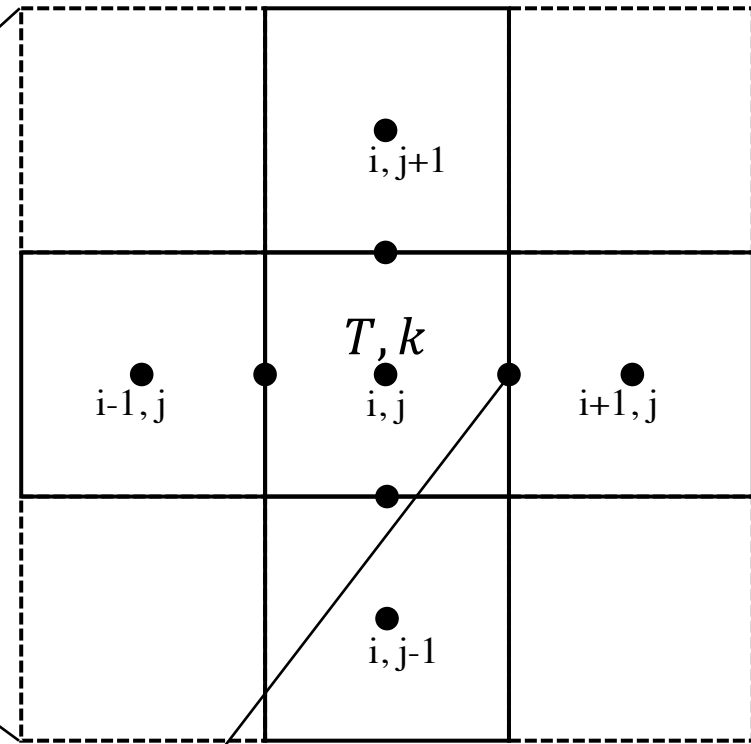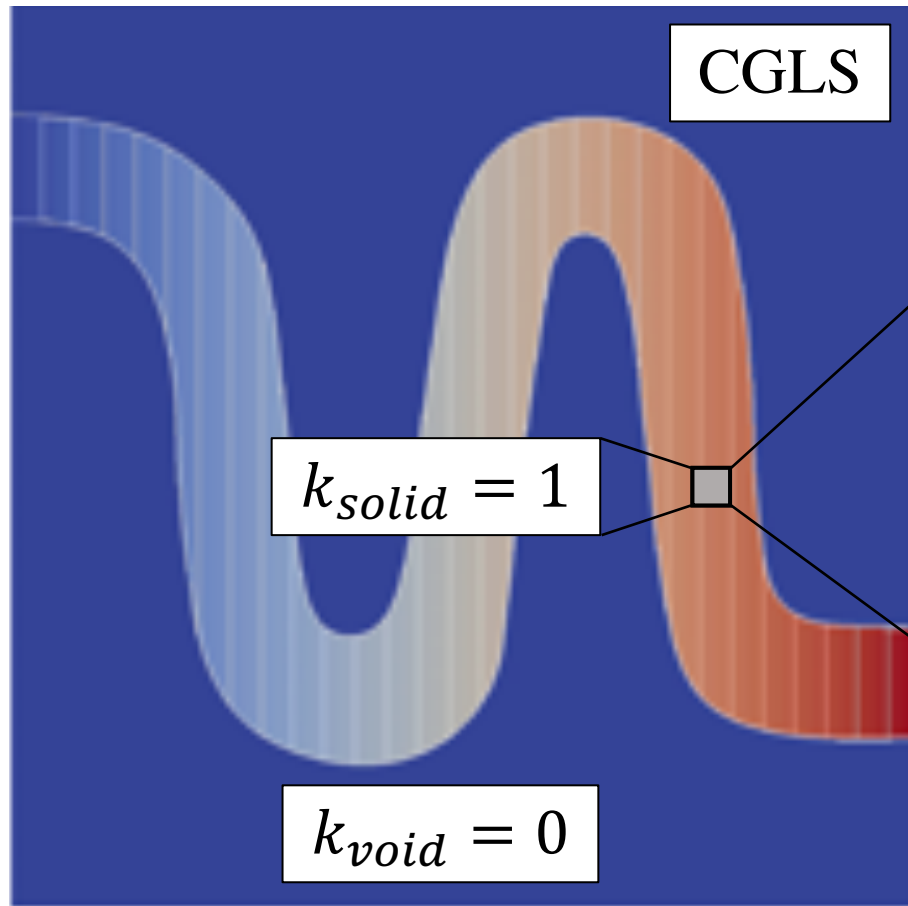
Ray Casting

$$\theta \in [0, 180°) \qquad \phi \in [0, 360°)$$

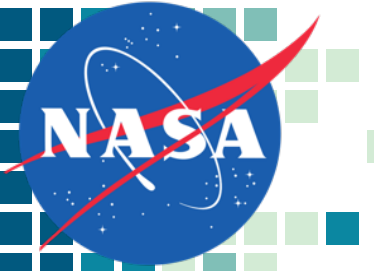$$N = \left(\frac{180°}{d\psi} - 1\right)\left(\frac{360°}{d\psi}\right) + 2$$
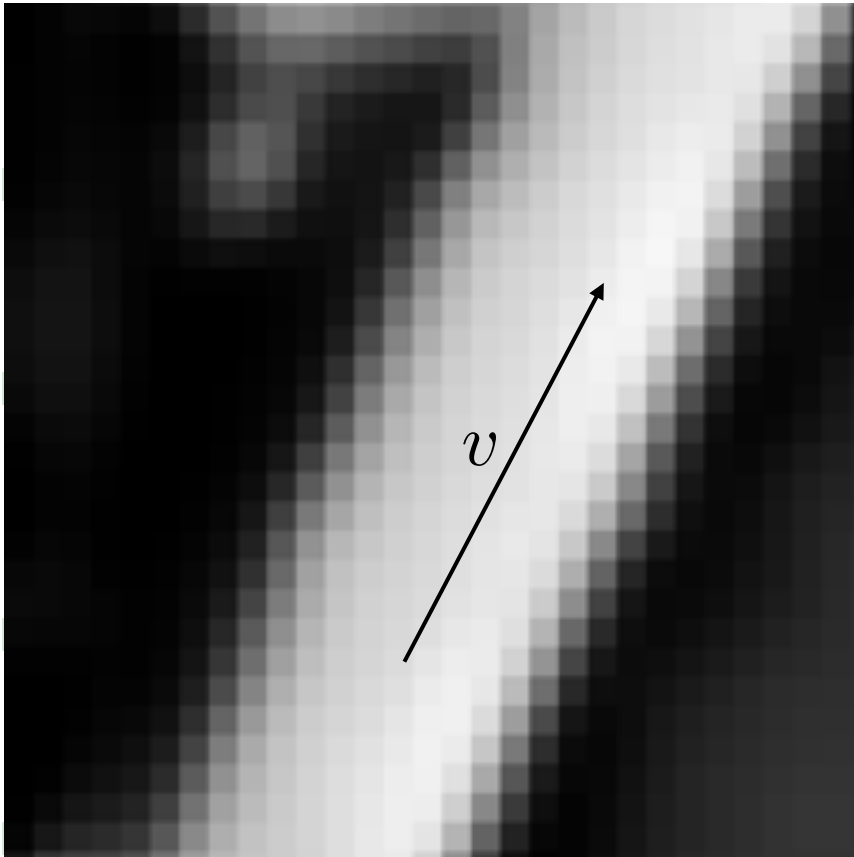
Artificial Flux

CGLS

$k_{solid} = 1$

$k_{void} = 0$

$$T_{i+1/2} = \frac{k_{i+1}}{k_i + k_{i+1}} T_{i+1} + \frac{k_i}{k_i + k_{i+1}} T_i$$
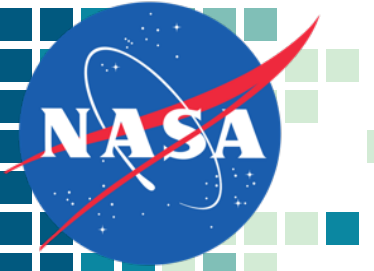
Structure Tensor

$$(I(x+v) - I(x))^2 \approx 0$$
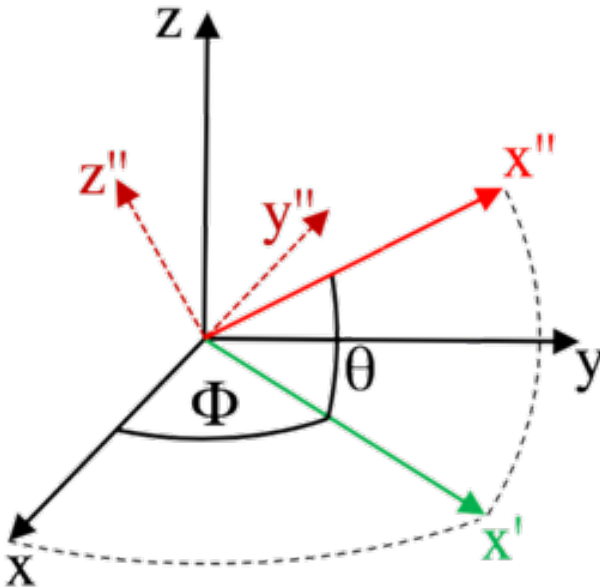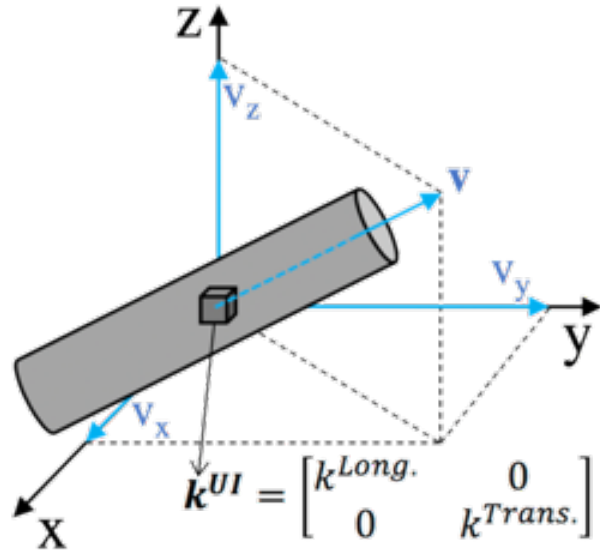
4 Steps:

1. $\nabla I_\sigma(x) = \nabla(\sigma * I(x))$

2. $\nabla I_\sigma \nabla I_\sigma^T = \begin{pmatrix} I_x^2 & I_x I_y & I_x I_z \\ I_x I_y & I_y^2 & I_y I_z \\ I_x I_z & I_y I_z & I_z^2 \end{pmatrix}$

3. $J_\rho(x) = \rho * (\nabla I_\sigma \nabla I_\sigma^T)$

4. Local orientation vector v is the eigenvector related to the smallest eigenvalue of $J_\rho(x)$
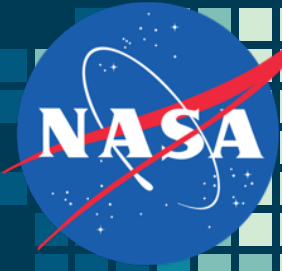
Conductivity Tensor Rotation

$$\boldsymbol{v} = v_x \boldsymbol{i} + v_y \boldsymbol{j} + v_z \boldsymbol{k}$$

$$\boldsymbol{k}'' = \begin{bmatrix} k^{Long.} & 0 & 0 \\ 0 & k^{Trans.} & 0 \\ 0 & 0 & k^{Trans.} \end{bmatrix}$$

$$\boldsymbol{k}^{UI} = \begin{bmatrix} k^{Long.} & 0 \\ 0 & k^{Trans.} \end{bmatrix}$$

$$\theta = \arcsin v_z \quad \phi = \arctan \frac{v_y}{v_x}$$

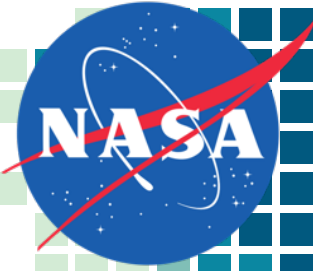$$\boldsymbol{q} = \underbrace{\left[\boldsymbol{R}^{-1} \boldsymbol{k}'' \boldsymbol{R} \right]}_{\boldsymbol{k}} \nabla T$$

$$\boldsymbol{R} = \begin{bmatrix} \cos\theta & 0 & -\sin\theta \\ 0 & 1 & 0 \\ \sin\theta & 0 & \cos\theta \end{bmatrix} \begin{bmatrix} \cos\phi & \sin\phi & 0 \\ -\sin\phi & \cos\phi & 0 \\ 0 & 0 & 1 \end{bmatrix}$$
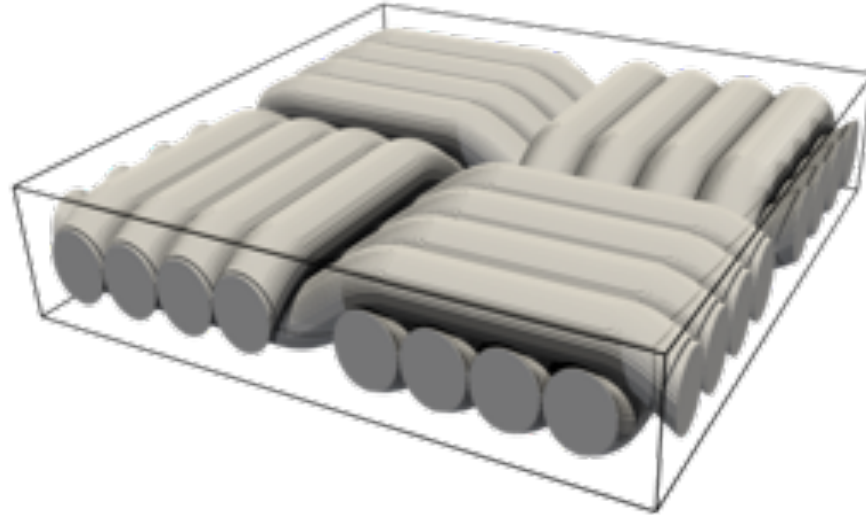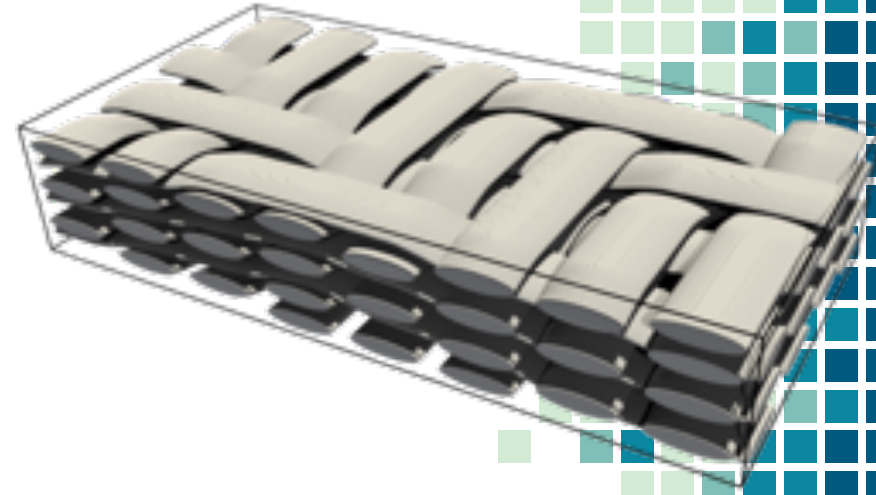
APPLICATION TO MATERIALS

Parametric Study

Artificial Straight Fibers

2D Weave

3D Weave

Methods' Inputs

Methods' Performance

Ray Casting (RC)

~~Ray angle separation $d\psi$~~

Artificial Flux (AF)

~~Solver Tolerance~~

Structure tensor (ST)
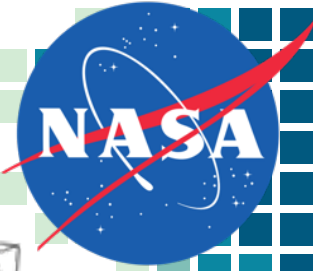
Kernel window sizes:
1. σ
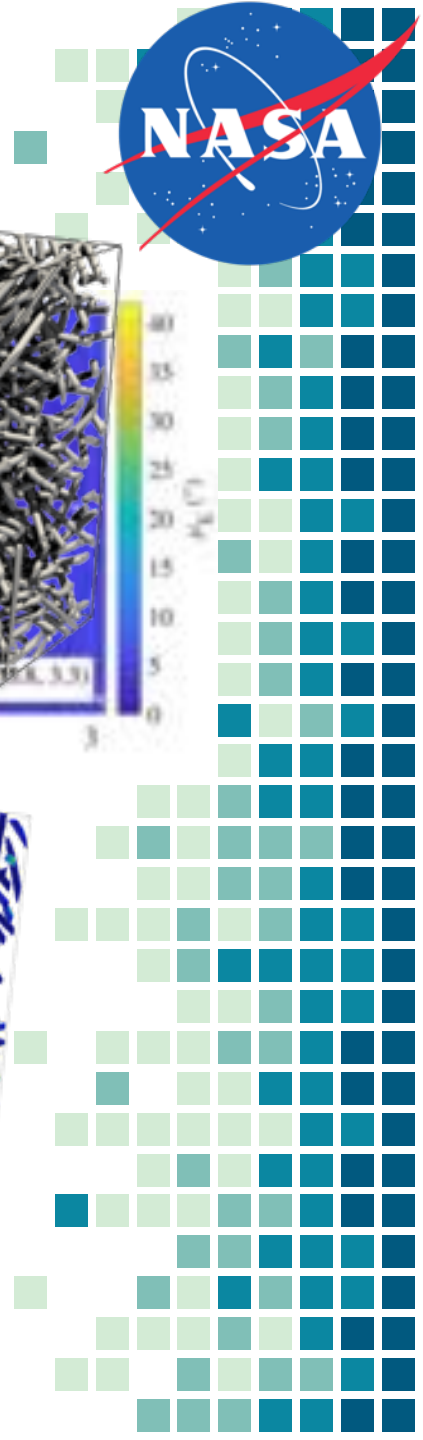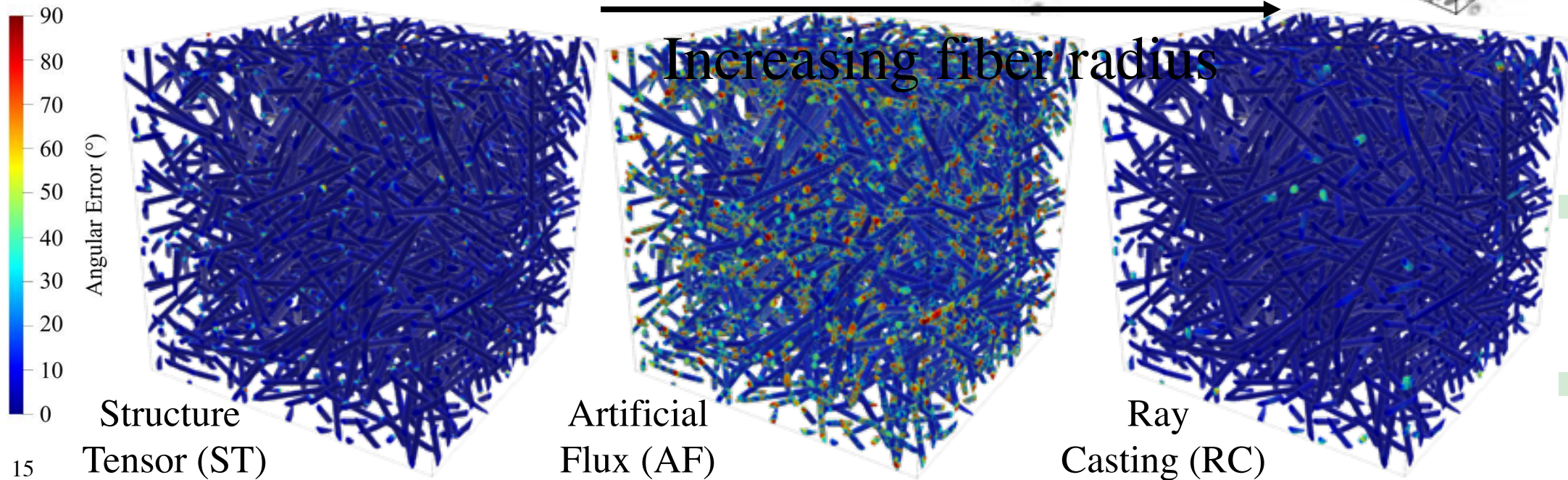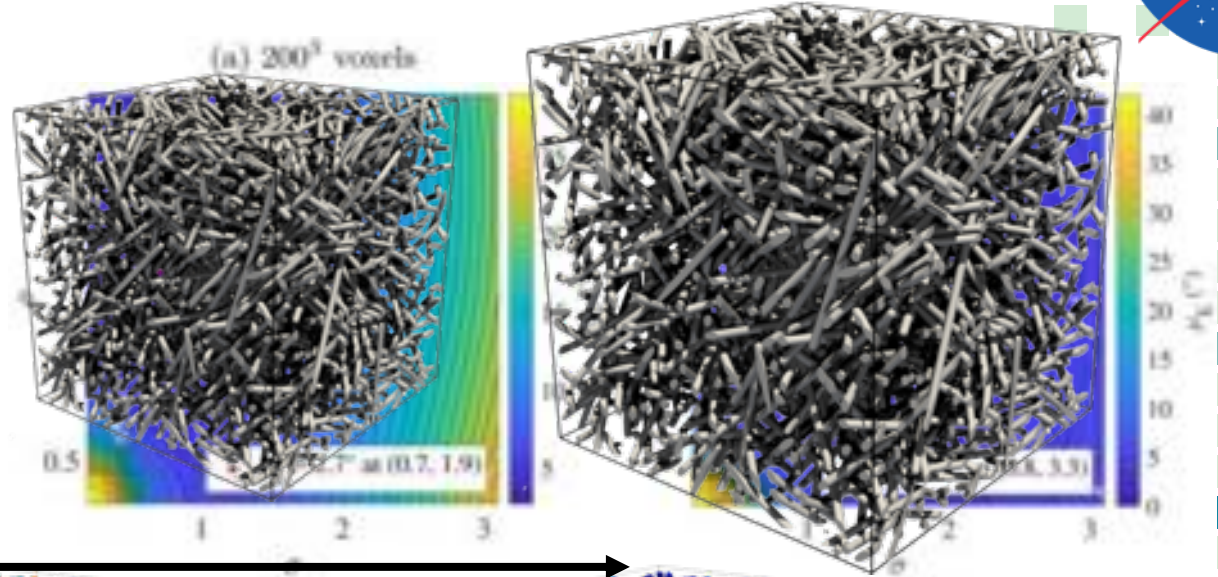2. ρ

Mean Angular Error

$$\mu_E = \sum_{n=1}^{N_{solid}} \frac{\alpha_n(x)}{N_{solid}}$$

Results on Artificial Fibrous Samples

Resolution (vox)	$\mu_{E,ST}(°)$	$\mu_{E,A}$
200^3		20
400^3		17
600^3		16
800^3	1.8	16.7

Increasing fiber radius

Structure Tensor (ST)

Artificial Flux (AF)

Ray Casting (RC)

Results on Real Fibrous Samples
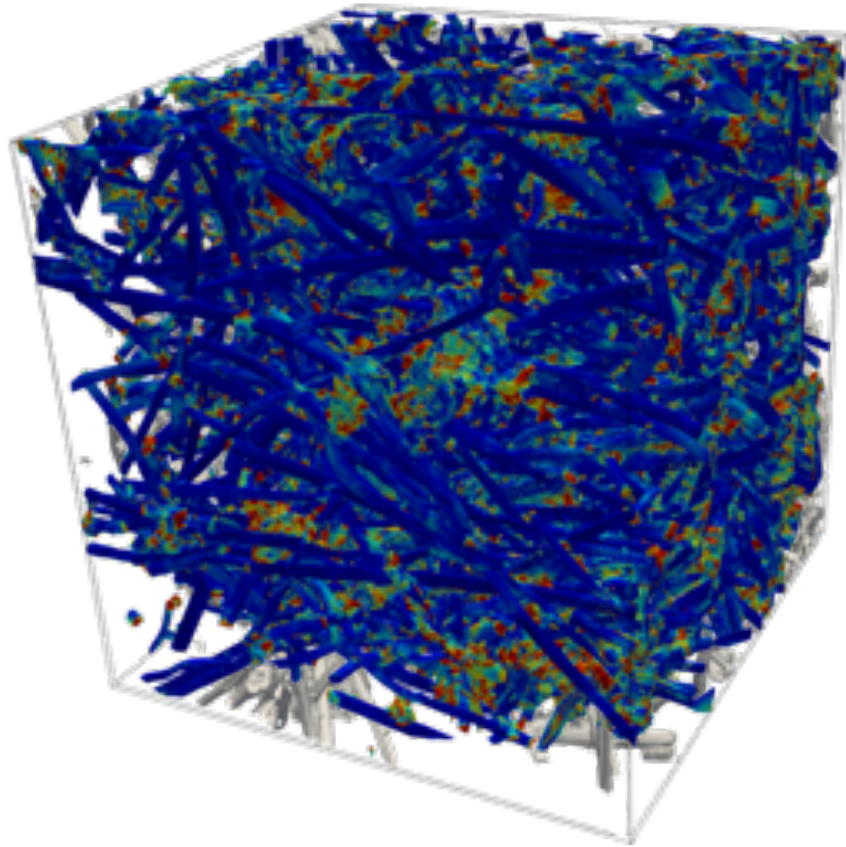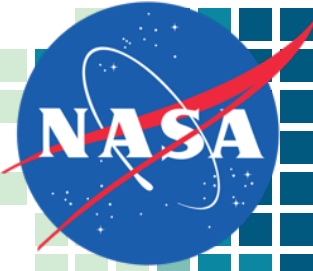
FiberForm™ 800³ voxels

$$\mu_\alpha = 21.6°$$

Structure Tensor
v.s.
Ray Casting
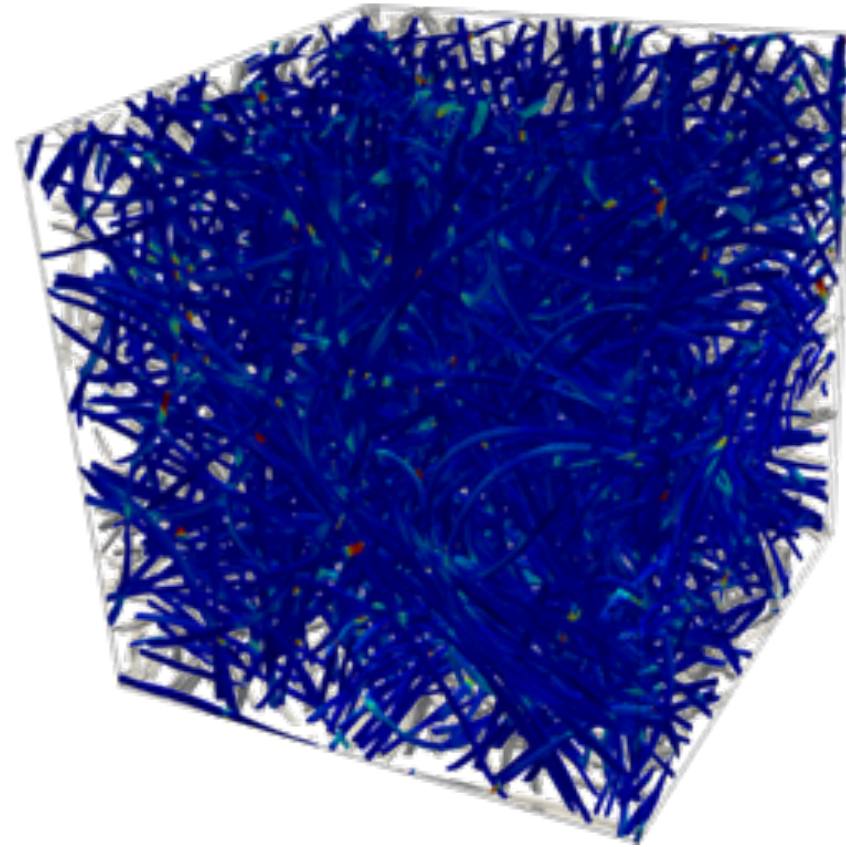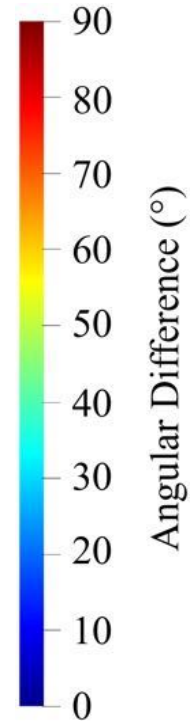
Morgan Felt 800³ voxels

$$\mu_\alpha = 8.5°$$
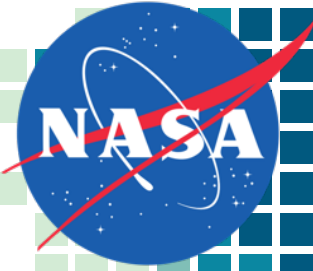
Results on Artificial Woven Samples

Design	Resolution (vox)	$\mu_{E,ST}(°)$	$\mu_{E,AF}(°)$	$\mu_{E,RC}(°)$
Circular Tows	$200^2 \times 50$	4.9	14.0	18.3
	$400^2 \times 100$	4.6	12.5	17.6
	$600^2 \times 150$	4.8	11.8	
	$800^2 \times 200$	5.1		
Elliptical Tows	$200 \times 400 \times 80$	30.1		
	$400 \times 800 \times 160$	25.9		
	$600 \times 1200 \times 240$	25.9		
	$800 \times 1600 \times 320$	26.5	15.6	

2D Weave

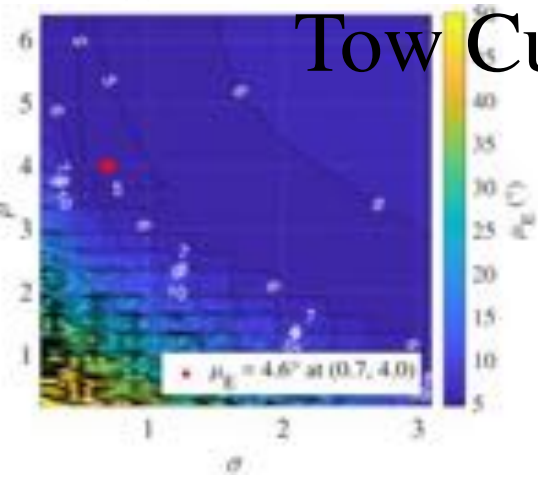3D Weave

Structure (ST)

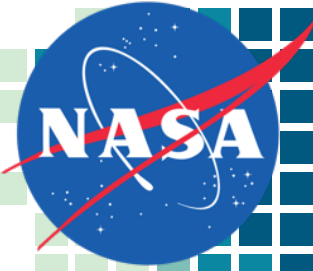Artificial Flux (AF)

Ray Casting (RC)
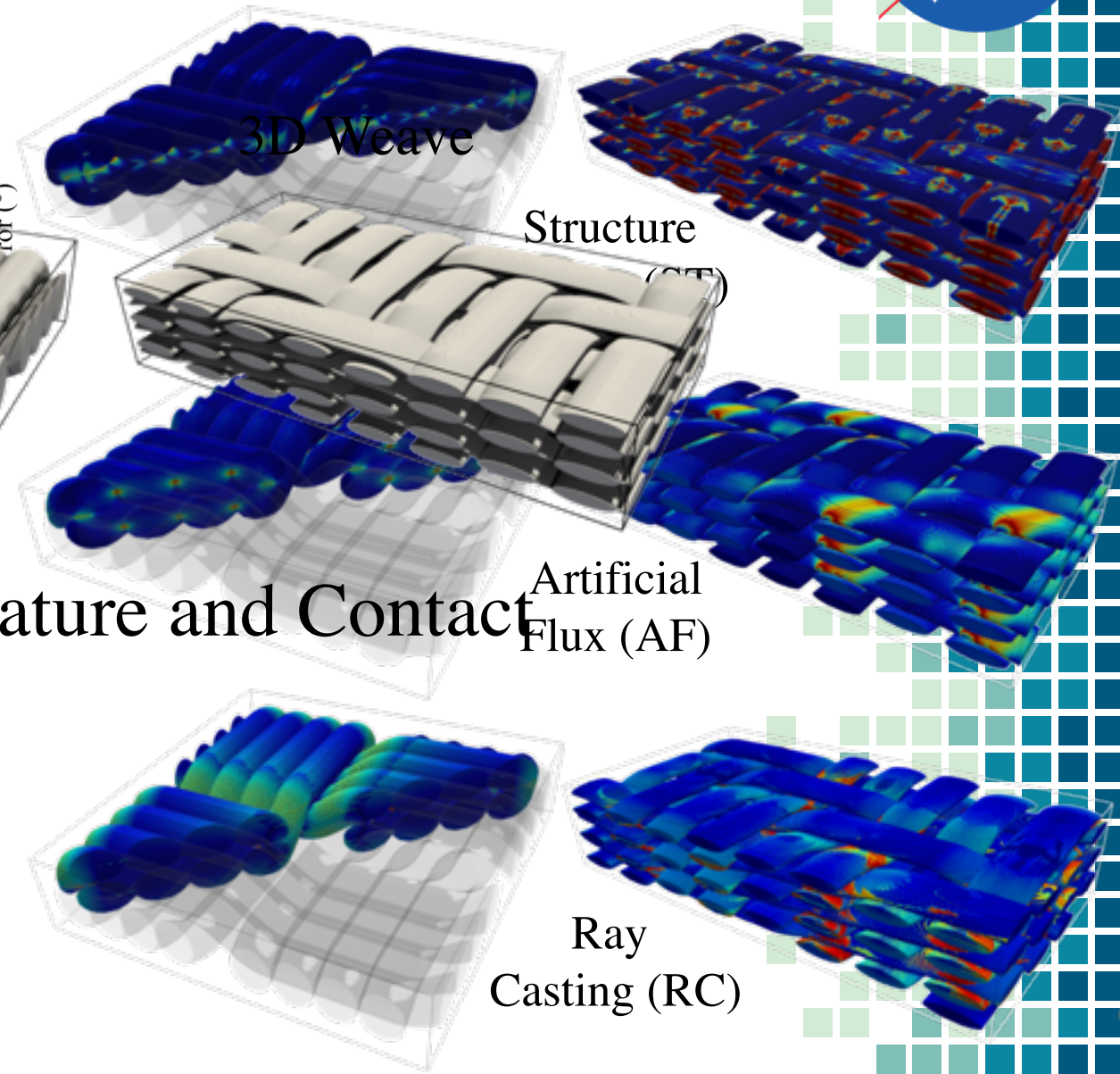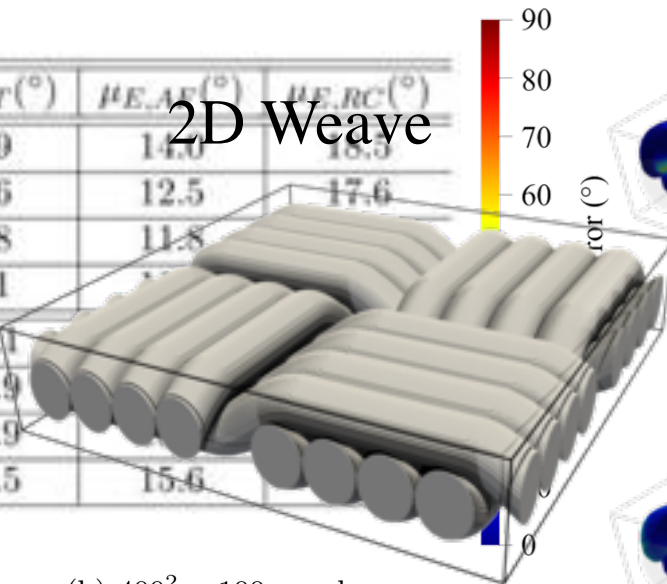
Tow Curvature and Contact

(a) $200^2 \times 50$ voxels

(b) $400^2 \times 100$ voxels

$\mu_E = 4.9°$ at $(0.7, 2.0)$

$\mu_E = 4.6°$ at $(0.7, 4.0)$
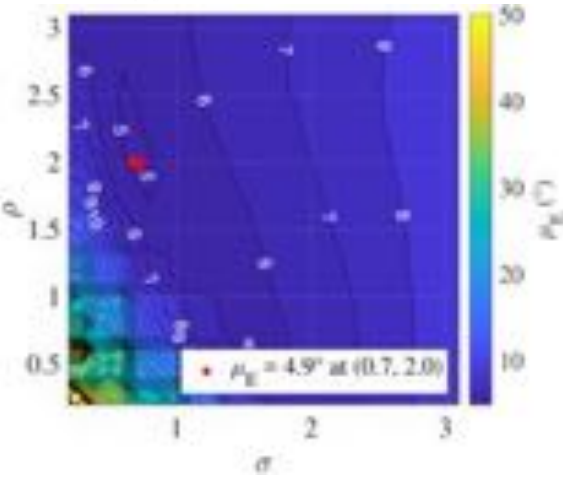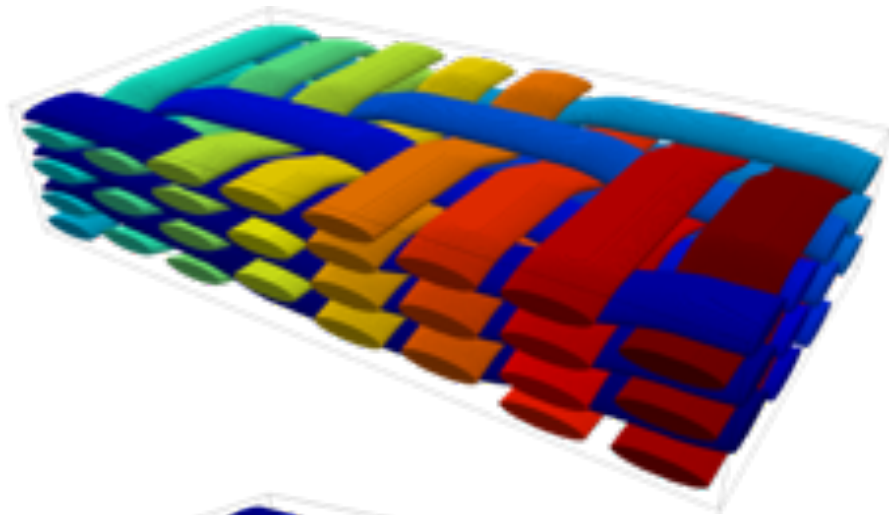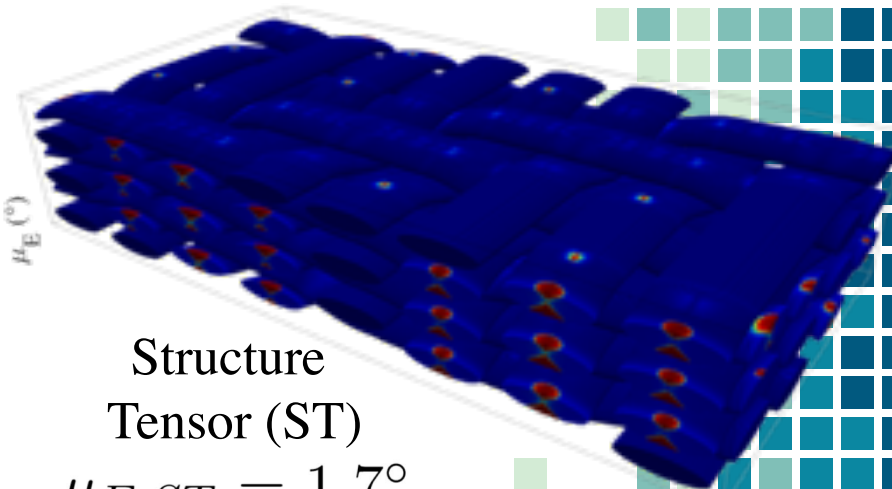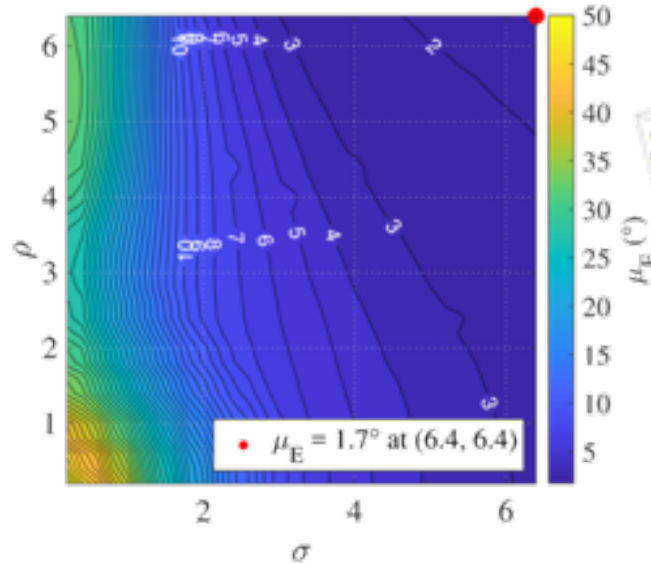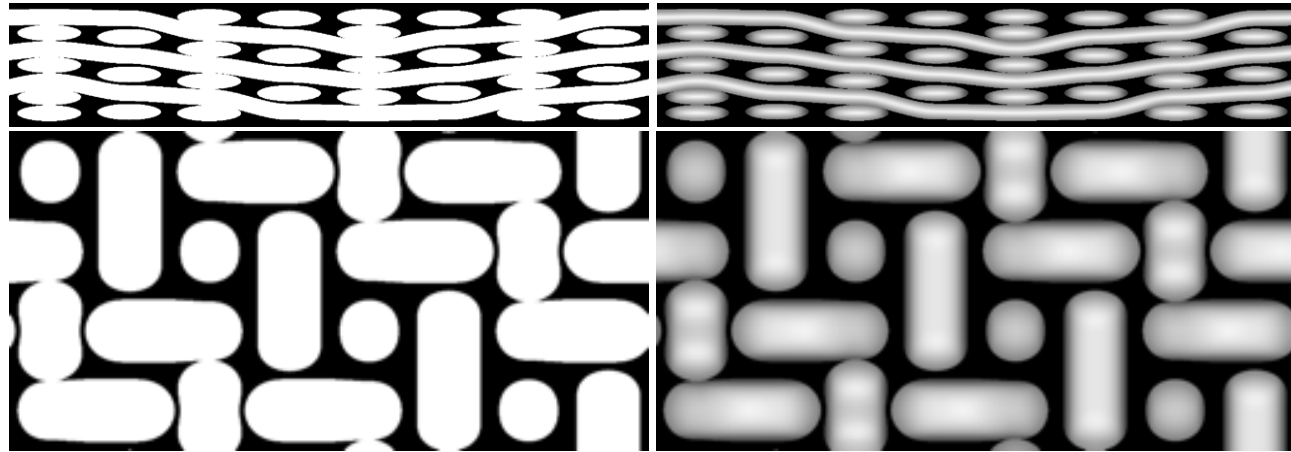
Improved Workflow for Weave Orientation

Individual tow segmentation

Mean Filtering

Artificial
Flux (AF)
$\mu_{E,AF} = 2.3°$
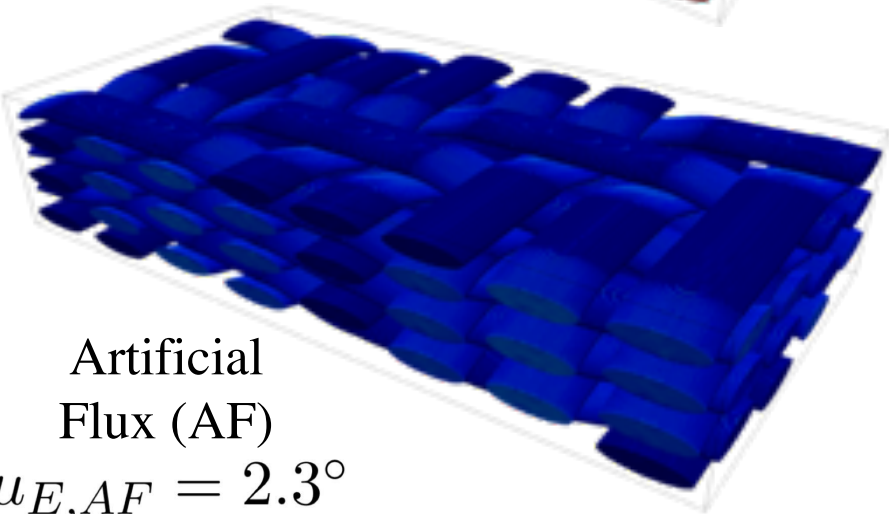
Structure
Tensor (ST)
$\mu_{E,ST} = 1.7°$

$\mu_E = 1.7°$ at (6.4, 6.4)

Real Woven Sample[1]
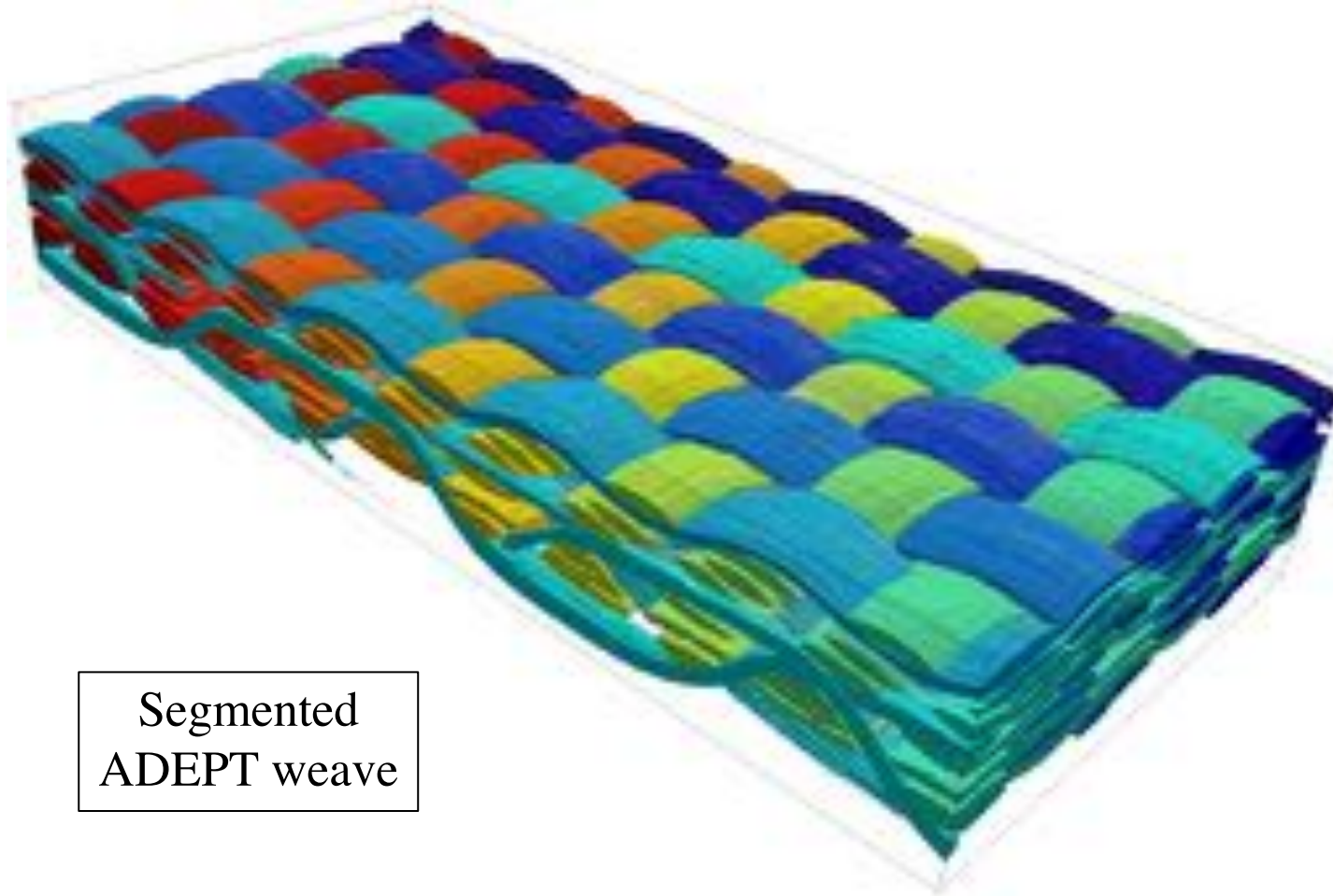
Segmented
ADEPT weave

[1] J. M. L. MacNeil, D. M. Ushizima, F. Panerai, N. N. Mansour, H. S. Barnard, D. Y. Parkinson, Interactive volumetric segmentation for textile micro-tomography data using wavelets and nonlocal means, *Statistical Analysis and Data Mining: The ASA Data Science Journal 12* (4) (2019) 338–353

19
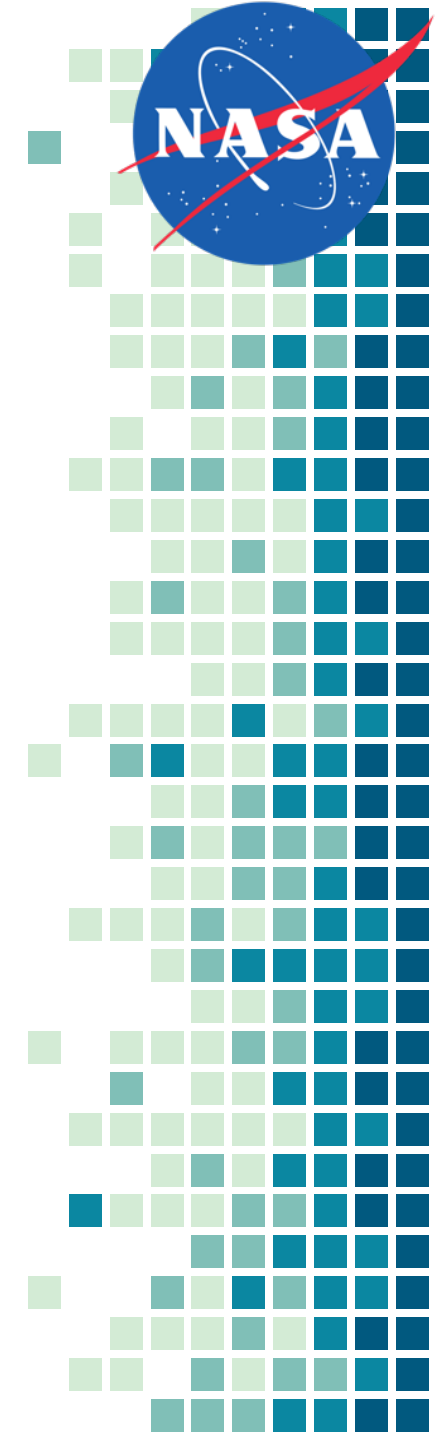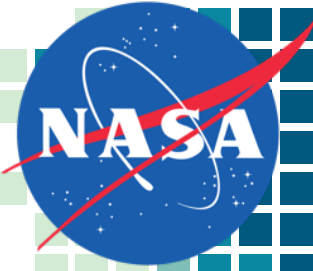
Summary

1. **Ray Casting:**

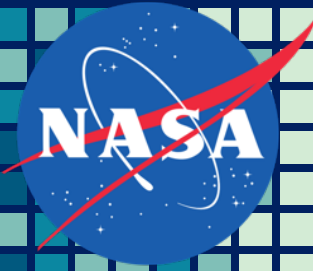   ➤ Performs well on artificial straight fibers ($\mu \sim 3 - 5°$) and similar to other methods on binarized woven structures ($\mu \sim 10 - 15°$). Slight improvement in new workflow ($\mu \sim 9°$)

   ➤ Limitation: affected by large fiber curvatures and computational expensive

2. **Artificial Flux:**

   ➤ Easy to use because independent on inputs. Performs similar to other methods on binarized weaves ($\mu \sim 15°$). Very accurate when using new workflow for woven materials ($\mu \sim 1 - 3°$)

   ➤ Limitation: Performs poorly on artificial straight fibers due to regions not being in the path of heat flux through the material ($\mu \sim 15 - 20°$)

3. **Structure Tensor:**

   ➤ Performs effectively on artificial straight fibers ($\mu \sim 1 - 5°$) and similar to other methods on binarized weaves ($\mu \sim 20°$). Very accurate when using new workflow for woven materials ($\mu \sim 1 - 2°$)

   ➤ Limitation: hard to define optimal window a priori. For high resolutions, window must be sufficiently large, which can be very expensive